Differential Effects of Interleukin-6 and -10 on Skeletal Muscle and Liver Insulin Action In Vivo

Hyo-Jeong Kim,[1] Takamasa Higashimori,[1] So-Young Park,[1] Hyejeong Choi,[1] Jianying Dong,[1] Yoon-Jung Kim,[1] Hye-Lim Noh,[1] You-Ree Cho,[1] Gary Cline,[1] Young-Bum Kim,[2] and Jason K. Kim[1]

The circulating level of the inflammatory cytokine interleukin (IL)-6 is elevated in various insulin-resistant states including type 2 diabetes, obesity, cancer, and HIV-associated lipodystrophy. To determine the role of IL-6 in the development of insulin resistance, we examined the effects of IL-6 treatment on whole-body insulin action and glucose metabolism in vivo during hyperinsulinemic-euglycemic clamps in awake mice. Pretreatment of IL-6 blunted insulin's ability to suppress hepatic glucose production and insulin-stimulated insulin receptor substrate (IRS)-2–associated phosphatidylinositol (PI) 3-kinase activity in liver. Acute IL-6 treatment also reduced insulin-stimulated glucose uptake in skeletal muscle, and this was associated with defects in insulin-stimulated IRS-1–associated PI 3-kinase activity and increases in fatty acyl-CoA levels in skeletal muscle. In contrast, we found that co-treatment of IL-10, a predominantly anti-inflammatory cytokine, prevented IL-6–induced defects in hepatic insulin action and signaling activity. Additionally, IL-10 co-treatment protected skeletal muscle from IL-6 and lipid-induced defects in insulin action and signaling activity, and these effects were associated with decreases in intramuscular fatty acyl-CoA levels. This is the first study to demonstrate that inflammatory cytokines IL-6 and IL-10 alter hepatic and skeletal muscle insulin action in vivo, and the mechanism may involve cytokine-induced alteration in intracellular fat contents. These findings implicate an important role of inflammatory cytokines in the pathogenesis of insulin resistance. *Diabetes* **53:1060–1067, 2004**

I nsulin resistance is a major characteristic of numerous metabolic disorders and pathological states including type 2 diabetes, obesity, cancer, and HIV-associated lipodystrophy syndrome (1–7). Despite its widely recognized significance, the molecular mecha-

nism by which insulin resistance occurs is unknown. Recent studies have shown that adipose tissue is an important endocrine organ capable of producing various hormones/cytokines, including adiponectin, leptin, resistin, tumor necrosis factor (TNF)-α, and interleukin (IL)-6, that may modulate glucose homeostasis, and alteration in their levels has been implicated in the pathogenesis of insulin resistance (8–14). IL-6 is a multifunctional cytokine that is produced and released by a wide variety of cell types, including macrophages, adipocytes, and skeletal muscle, and has been shown to alter glucose metabolism in hepatocytes and adipocytes (15–19). Furthermore, Fernandez-Real et al. (20) recently demonstrated that a polymorphism of the IL-6 gene at position −174 was associated with insulin resistance, whereas the C-174G promoter polymorphism of the IL-6 gene was shown to affect insulin sensitivity in humans (21). Although the role of IL-6 has been previously examined in isolated hepatocytes and adipocytes, their effects on skeletal muscle insulin action, the major site of glucose disposal and of defects in the insulin-resistant state (22), have not been addressed. Thus, the present study examined the effects of acute IL-6 treatment on whole-body and tissue-specific insulin action and glucose metabolism in vivo.

Furthermore, our recent study has shown that a high-dose treatment of anti-inflammatory salicylate prevented lipid-induced insulin resistance in skeletal muscle, and the underlying mechanism involved salicylate-mediated inhibition of IκB kinase (IKK)-β (23,24). This observation was further supported by our findings that IKK-β null mice were protected from lipid-induced insulin resistance (23). In this regard, IL-10, a predominantly anti-inflammatory cytokine, has been shown to inhibit TNF-α–induced activation of NF-κB by inhibiting IKK activity in human monocytic cell lines (25). Moreover, Van Exel et al. (26) recently showed in the Leiden 85-Plus Study that a low IL-10 production capacity was associated with hyperglycemia, high HbA$_{1c}$, dyslipidemia, and diabetes. In light of these findings, we also examined the effects of co-treatment of IL-10 and lipid infusion or IL-6 on insulin action and glucose metabolism in vivo.

RESEARCH DESIGN AND METHODS

Animals and surgery. Male C57BL/6 mice at ~12 weeks of age were obtained from The Jackson Laboratory and studied after 2–3 weeks of acclimatization. Mice were housed under controlled temperature (23°C) and lighting (12 h of light, 0700–1900; 12 h of dark, 1900–0700) with free access to water and standard mouse diet. All procedures were approved by the Yale University Animal Care and Use Committee. At least 4 days before hyperinsulinemic-euglycemic clamp experiments, mice were anesthetized with an intraperitoneal injection of ketamine (100 mg/kg body wt) and xylazine (10 mg/kg body

wt), and an indwelling catheter was inserted in the right internal jugular vein as previously described (27). On the day of clamp experiment, a three-way connector was attached to the jugular vein catheter to intravenously deliver solutions (e.g., glucose, insulin), and the blood samples were obtained from the tail vessel (27).

Hyperinsulinemic-euglycemic clamps to assess insulin action and signaling in vivo. After an overnight fast, saline (control, $n = 8$) or mouse recombinant IL-6 (0.5 μg/h, $n = 5$; Sigma, St. Louis, MO) was infused for 2 h of the pretreatment period and a blood sample (60 μl) was collected at the end for the measurements of glucose, insulin, and fatty acids. The IL-6 pretreatment period was followed by a 2-h hyperinsulinemic-euglycemic clamp with a primed-continuous infusion of human insulin (Humulin; Eli Lilly, Indianapolis, IN) at a rate of 15 pmol · kg^{-1} · min^{-1} to raise plasma insulin within a physiological range and continuous IL-6 infusion. Blood samples (20 μl) were collected at 20-min intervals for the immediate measurement of plasma glucose concentration, and 20% glucose was infused at variable rates to maintain plasma glucose at basal concentrations. Basal and insulin-stimulated whole-body glucose turnover was estimated with a continuous infusion of [3-^{3}H]glucose (Perkin Elmer Life and Analytical Sciences, Boston, MA) during the pretreatment period (0.05 μCi/min) and throughout the clamps (0.1 μCi/min). All infusions were performed using microdialysis pumps (CMA/ Microdialysis, North Chelmsford, MA). To estimate insulin-stimulated glucose uptake in individual tissues, 2-deoxy-D-[1-^{14}C]glucose (2-[^{14}C]DG) (Perkin Elmer) was administered as a bolus (10 μCi) at 75 min after the start of clamps as previously described (27). Blood samples were taken during and at the end of clamps for measurement of plasma [^{3}H]glucose, ^{3}H$_2$O, 2-[^{14}C]DG concentrations, insulin, and/or fatty acids concentrations (27). At the end of the clamps, mice were anesthetized with sodium pentobarbital injection. Within 5 min, three muscles (gastrocnemius, tibialis anterior, and quadriceps) from both hindlimbs, epididymal white adipose tissue, interscapular brown adipose tissue, liver, and heart were taken as previously described (27).

Biochemical assays and calculation. The glucose concentration during the clamps was analyzed using 10 μl plasma by a glucose oxidase method on a Beckman Glucose Analyzer 2 (Beckman, Fullerton, CA). Plasma insulin concentration was measured by radioimmunoassay using kits from Linco Research (St. Charles, MO). Plasma fatty acid concentration was determined using an acyl-CoA oxidase-based colorimetric kit (Wako Chemicals, Richmond, VA). Plasma concentrations of [3-^{3}H]glucose, 2-[^{14}C]DG, and ^{3}H$_2$O were determined after deproteinization of plasma samples as previously described (27). The radioactivity of ^{3}H in tissue glycogen was determined by digesting tissue samples in KOH and precipitating glycogen with ethanol. For the determination of tissue 2-[^{14}C]DG-6-phosphate content, tissue samples were homogenized, and the supernatants were subjected to an ion-exchange column to separate 2-[^{14}C]DG-6-phosphate from 2-[^{14}C]DG (27).

Rates of basal and insulin-stimulated whole-body glucose turnover were determined as the ratio of the [^{3}H]glucose infusion rate (disintegrations per minute [dpm]) to the specific activity of plasma glucose (dpm/μmol) at the end of the basal period and during the final 30 min of the clamps, respectively. Hepatic glucose production (HGP) during the clamps was determined by subtracting the steady-state glucose infusion rate from the whole-body glucose turnover rate. Whole-body glycolysis and glycogen/lipid synthesis were calculated as previously described (27). Glucose uptake in individual tissues was calculated from the plasma 2-[^{14}C]DG profile, which was fitted with a double exponential or linear curve using MLAB (Civilized Software, Bethesda, MD) and tissue 2-[^{14}C]DG-6-phosphate content. Skeletal muscle glycolysis and glycogen synthesis were calculated as previously described (27).

Insulin signaling analysis. Skeletal muscle (gastrocnemius) and liver samples were obtained at the end of the clamps to measure in vivo activities of insulin receptor substrate (IRS)-1– and IRS-2–associated phosphatidylinositol (PI) 3-kinase, respectively. These activities were assessed by immunoprecipitating tissue lysates with polyclonal IRS-1/IRS-2 antibodies (Upstate Biotechnology, Lake Placid, NY) coupled with protein A-sepharose beads (Sigma) and assessing the incorporation of ^{32}P into PI to yield PI-3-monophosphate. The immune complex was washed, and the activity was determined as previously described (28). Insulin-stimulated activity of protein kinase C (PKC)-λ/ζ was determined by immunoprecipitating tissue lysates with a polyclonal PKC-ζ antibody (Santa Cruz Biotechnology, Santa Cruz, CA) that recognized both PKC-λ and -ζ, coupled with protein A-sepharose beads as previously described (28). Insulin-stimulated Akt activity was determined by immunoprecipitating tissue lysates with a polyclonal Akt antibody (Upstate Biotechnology) that recognized both Akt1 and Akt2, coupled with protein G-sepharose beads (Amersham Pharmacia Biotechnology, Piscataway, NJ) as previously described (28).

Measurements of phospho-STAT3 expression and fatty acyl-CoA in skeletal muscle and liver. To determine STAT3 tyrosine phosphorylation in IL-6–treated skeletal muscle, tissue samples were obtained after 10-min postintraperitoneal IL-6 injection (1 μg) or 2-h intravenous IL-6 infusion (0.5 μg/h). Muscle lysates (gastrocnemius) were resolved by SDS-PAGE (8% gel) and transferred to nitrocellulose membranes. The nitrocellulose membranes were blocked and incubated with phospho-specific STAT3 (Tyr705) polyclonal antibody (Cell Signaling, Beverly, MA). The membranes were washed and incubated with horseradish peroxidase secondary antibody (Amersham Pharmaceuticals, Arlington Heights, IL), and the bands were visualized using the enhanced chemiluminescence system (Amersham Pharmaceuticals).

To determine the intramuscular and intrahepatic concentrations of fatty acyl-CoA using liquid chromatography tandem mass spectrometry, skeletal muscle (quadriceps) and liver samples were homogenized and prepared using a modified method of Bligh and Dyer (29). A PE Sciex API 3000 tandem mass spectrometer (Applied Biosystems, Foster City, CA) interfaced with the TurboIonSpray ionization source was used for the analysis. The intracellular concentrations of long-chain fatty acyl-CoAs (C16:0, C16:1, C18:0, C18:1, C18:2, and C18:3) were detected in negative electrospray mode, and C17 CoA ester was used as an internal standard. The doubly charged ions of these compounds were transmitted, and singly charged product ions were quantified in multiple reaction mode.

Effects of IL-10 co-treatment on IL-6 and lipid-induced insulin resistance in vivo. To examine the effects of IL-10 on IL-6–induced insulin resistance, mouse recombinant IL-10 (0.5 μg/h; Sigma) was co-infused with IL-6 (0.5 μg/h) for 2 h of the pretreatment period ($n = 7$), and a 2-h hyperinsulinemic-euglycemic clamp was conducted in awake mice. Moreover, the effects of IL-10 on lipid-induced insulin resistance were examined by infusing lipid (5 ml · kg^{-1} · h^{-1}, Liposyn II, triglyceride emulsion, 20% wt/vol; Abbott, Chicago) and heparin (6 units/h) with or without IL-10 (0.2 μg/h) for 5 h ($n = 5$ for each group), and the clamp experiment was conducted in awake mice. The effects of IL-10 treatment alone on insulin action were determined in an additional group of mice treated with a 2-h infusion of saline ($n = 6$) or IL-10 (0.5 μg/h, $n = 7$) followed by clamp experiments.

For insulin-signaling assays (i.e., IRS-1/IRS-2–associated PI 3-kinase, PKC-λ/ζ, and Akt/protein kinase B [PKB] activities), skeletal muscle (gastrocnemius) and liver samples were obtained at the end of clamp experiments. For phospho-STAT3 expression and fatty acyl-CoA levels, skeletal muscle (gastrocnemius and quadriceps, respectively) and/or liver samples were obtained after a 2-h intravenous co-infusion of IL-10 and IL-6 (0.5 μg/h for each) or 5-h co-infusion of IL-10 (0.2 μg/h) and lipid (5 ml · kg^{-1} · h^{-1}).

Statistical analysis. Data are expressed as means ± SE. The significance of the difference in mean values among control, IL-6 treated, IL-6/IL-10 co-treated, lipid-infused, and lipid/IL-10 co-treated groups was evaluated using the Duncan's multiple range test. The significance of the difference in mean values between control and IL-10–treated mice was evaluated using the Student's t test.

RESULTS

IL-6 decreased skeletal muscle insulin action and signaling in vivo. IL-6 treatment did not affect basal concentrations of glucose, insulin, and fatty acids compared with the controls (Table 1). Although previous studies have shown the inhibitory effects of IL-6 on pancreatic β-cell function (30,31), our 2-h infusion of IL-6 did not affect circulating insulin levels. Furthermore, previous studies have shown that IL-6 affected the hypothalamus-pituitary-adrenal cortex axis and increased circulating cortocosterone levels in humans (12,32). However, our findings of normal glucose and fatty acids concentrations after acute IL-6 treatment suggested that the dose of IL-6 used in this study did not significantly affect the hypothalamus-pituitary-adrenal cortex axis. During the clamp experiments, the plasma insulin concentration was raised to ~450 pmol/l, whereas the plasma glucose concentration was maintained at ~7 mmol/l by a variable infusion of glucose in both groups (Table 2).

The rates of glucose infusion required to maintain euglycemia increased rapidly in the controls and reached a steady state within 90 min. There was a markedly blunted insulin response during the hyperinsulinemic-euglycemic

TABLE 1
Metabolic parameters during the basal period (after pretreatment) in control (saline), IL-6–treated, IL-6– and IL-10–co-treated, lipid-infused, and lipid- and IL-10–co-treated groups

			Basal period		
	n	Body weight (g)	Plasma glucose (mmol/l)	Plasma insulin (pmol/l)	Plasma fatty acids (mmol/l)
Control	8	24 ± 1	9.1 ± 0.5	130 ± 15	1.2 ± 0.1
IL-6–treated	5	22 ± 2	7.9 ± 0.5	119 ± 29	0.9 ± 0.1
IL-6– and IL-10–co-treated	7	22 ± 0	7.9 ± 0.7	$86 \pm 10^*$	1.1 ± 0.1
Lipid-infused	5	27 ± 1	$6.9 \pm 0.4^*$	110 ± 18	$2.1 \pm 0.5^*$
Lipid- and IL-10–co-treated	5	27 ± 2	$7.2 \pm 0.3^*$	92 ± 15	$1.9 \pm 0.2^*$

Data are means $\pm$ SE. $*P < 0.05$ vs. control mice by Duncan's multiple range test.

clamp studies in the IL-6–treated mice, as reflected by a significantly lower steady-state glucose infusion rate (Table 2). Insulin-stimulated whole-body glucose turnover was decreased by ~25% after IL-6 treatment (144 ± 5 vs. 186 ± 12 $\mu mol \cdot kg^{-1} \cdot min^{-1}$ in the controls) (Fig. 1*A*). The rate of insulin-stimulated glucose uptake in skeletal muscle in vivo was assessed using 2-[^{14}C]DG injection during clamps in awake mice. The IL-6–induced whole-body insulin resistance was mostly accounted for by 40% decreases in insulin-stimulated skeletal muscle (gastrocnemius) glucose uptake (127 ± 14 vs. 218 ± 23 nmol $\cdot g^{-1} \cdot min^{-1}$ in the IL-6–treated mice vs. controls) (Fig. 1*B*). Insulin-stimulated whole-body glycolysis was significantly reduced, whereas whole-body glycogen/lipid synthesis showed a tendency to decrease after IL-6 treatment (Fig. 2*A* and *B*). The pattern of changes in skeletal muscle glucose metabolic flux paralleled that in whole-body glucose metabolism after IL-6 treatment (Fig. 2*C* and *D*). These results demonstrated that IL-6 treatment caused significant impairment in skeletal muscle insulin action in vivo.

Recent studies in *IRS-1* and *IRS-2* gene–disrupted mice have suggested that IRS-1 is important in insulin activation of muscle glucose metabolism (i.e., insulin-stimulated glucose transport and glycogen synthase activity), whereas IRS-2 is more important in mediating insulin activation of hepatic glucose metabolism (i.e., insulin-mediated suppression of basal HGP) (1,33). IL-6 treatment significantly reduced insulin-stimulated IRS-1–associated PI 3-kinase activity (39 ± 11 vs. 148 ± 9 arbitrary units in the IL-6–treated mice vs. controls), a key intracellular media-

TABLE 2
Metabolic parameters during hyperinsulinemic-euglycemic clamp periods in control (saline), IL-6–treated, IL-6– and IL-10–co-treated, lipid-infused, and lipid- and IL-10–co-treated groups

	Clamp period		
	Plasma glucose (mmol/l)	Plasma insulin (pmol/l)	Glucose infusion rate ($\mu mol \cdot kg^{-1} \cdot min^{-1}$)
Control	7.1 ± 0.2	409 ± 22	183 ± 11
IL-6–treated	7.0 ± 0.7	432 ± 52	$88 \pm 12^*$
IL-6– and IL-10–co-treated	7.1 ± 0.4	420 ± 16	191 ± 14
Lipid-infused	6.4 ± 0.2	427 ± 56	$140 \pm 6^*$
Lipid- and IL-10–co-treated	6.6 ± 0.4	442 ± 61	180 ± 17

Data are means $\pm$ SE. $*P < 0.05$ vs. control mice by Duncan's multiple range test.

tor of insulin signaling in skeletal muscle (Fig. 1*C*). These findings demonstrate that IL-6–induced skeletal muscle insulin resistance was most likely secondary to IL-6–induced defects in skeletal muscle insulin signaling. In contrast, insulin-stimulated activities of PKC-λ/ζ and Akt/PKB were not significantly altered among groups (7.0 ± 0.6 vs. 8.5 ± 1.1 arbitrary units for PKC-λ/ζ activity and 537 ± 120 vs. 483 ± 105 arbitrary units for Akt/PKB activity in the IL-6–treated mice vs. controls). Interestingly, IL-6 treatment significantly raised intramuscular total fatty acyl-CoA levels (sum of C16:0, C16:1, C18:0, C18:1, C18:2, and C18:3) in the skeletal muscle (quadriceps) compared with the controls (20 ± 4 vs. 8 ± 4 nmol/g in the IL-6–treated mice vs. controls) (Fig. 1*D*). Furthermore, IL-6 treatment increased tyrosine phosphorylation of STAT3 in skeletal muscle, indicating that the effect of IL-6 on skeletal muscle was mediated by IL-6–induced activation of the gp130 complex (Fig. 3).

IL-6–induced hepatic insulin resistance in vivo. The rates of basal HGP were not different among the groups, but insulin's ability to suppress basal HGP was significantly reduced after IL-6 treatment, reflecting IL-6–induced hepatic insulin resistance (57 ± 13 vs. 3 ± 8 $\mu mol \cdot kg^{-1} \cdot min^{-1}$ for clamp HGP in the IL-6–treated mice vs. controls) (Fig. 4*A* and *B*). This is the first in vivo demonstration of insulin resistance induced by IL-6 treatment in mice and supports previous in vitro findings in hepatocytes (17). Insulin-stimulated IRS-2–associated PI 3-kinase activity in liver was decreased by 50% after IL-6 treatment (508 ± 107 vs. 935 ± 79 arbitrary units in the IL-6–treated mice vs. controls) (Fig. 4*C*). In contrast to the findings in skeletal muscle, intrahepatic fatty acyl-CoA levels were reduced after IL-6 treatment (Fig. 4*D*).

IL-10 prevented IL-6–induced insulin resistance in skeletal muscle and liver in vivo. We examined the effects of 2-h treatment of IL-10 and 2-h co-treatment of IL-10 and IL-6 on in vivo insulin action during hyperinsulinemic-euglycemic clamps in awake mice. Plasma glucose concentrations after saline or IL-10 treatment did not differ among groups (7.8 ± 0.5 or 8.4 ± 0.5 mmol/l, respectively). Steady-state rates of glucose infusion as well as hepatic and peripheral insulin actions were not affected by IL-10 treatment (Fig. 5). Furthermore, plasma glucose, insulin, and fatty acids concentrations during basal or clamp periods did not differ after co-treatment of IL-10 and IL-6 compared with the controls or IL-6–treated mice (Tables 1 and 2). Remarkably, IL-10 co-treatment completely restored IL-6–induced blunted rates of glucose infusion
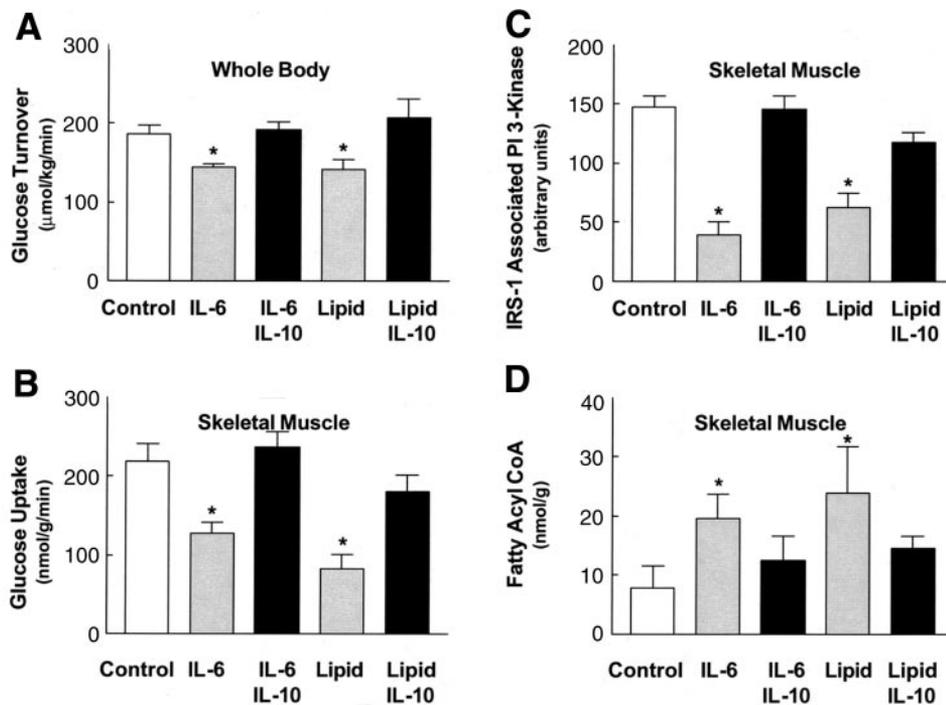
FIG. 1. Whole-body and skeletal muscle insulin action and fatty acyl-CoA levels in the control, IL-6, IL-6/IL-10, lipid, and lipid/IL-10 mice. *A*: Insulin-stimulated whole-body glucose turnover in vivo. *B*: Insulin-stimulated glucose uptake in skeletal muscle (gastrocnemius) in vivo. *C*: Insulin-stimulated IRS-1–associated PI 3-kinase activity in skeletal muscle (gastrocnemius). *D*: Intramuscular (quadriceps) fatty acyl-CoA levels. Values are means ± SE for five to eight experiments. *$P < 0.05$ vs. control mice.

during clamps (Table 2). Insulin-stimulated whole-body glucose turnover was normalized after IL-10 co-treatment (191 ± 10 μmol · kg^{-1} · min^{-1}) compared with the IL-6–treated mice, and this was accounted for by increases in insulin-stimulated skeletal muscle glucose uptake after IL-10 co-treatment (237 ± 20 nmol · g^{-1} · min^{-1}) (Fig. 1*A* and *B*). Similarly, rates of insulin-stimulated whole-body glycogen/lipid synthesis and skeletal muscle glycolysis were increased after IL-10 co-treatment compared with the IL-6–treated mice (Fig. 2*B* and *C*).

The protective effects of IL-10 on IL-6–induced skeletal muscle insulin resistance were secondary to their effects on skeletal muscle insulin signaling. After IL-10 co-treat-

ment, insulin-stimulated IRS-1–associated PI 3-kinase activity was significantly increased compared with the IL-6–treated mice (Fig. 1*C*). These changes in skeletal muscle insulin action and signaling were associated with significantly lower intramuscular fatty acyl-CoA levels in the IL-10 co-treated mice (13 ± 4 nmol/g) compared with the IL-6–treated mice (Fig. 1*D*). Furthermore, similar to the protective effects of IL-10 on IL-6–induced skeletal muscle insulin resistance, insulin's ability to suppress basal HGP (1 ± 5 μmol · kg^{-1} · min^{-1} for clamp HGP) and insulin-mediated IRS-2–associated PI 3-kinase activity ($1,023 \pm 239$ arbitrary units) were normalized after IL-10 co-treatment (Fig. 4*B* and *C*). Intrahepatic fatty acyl-CoA levels
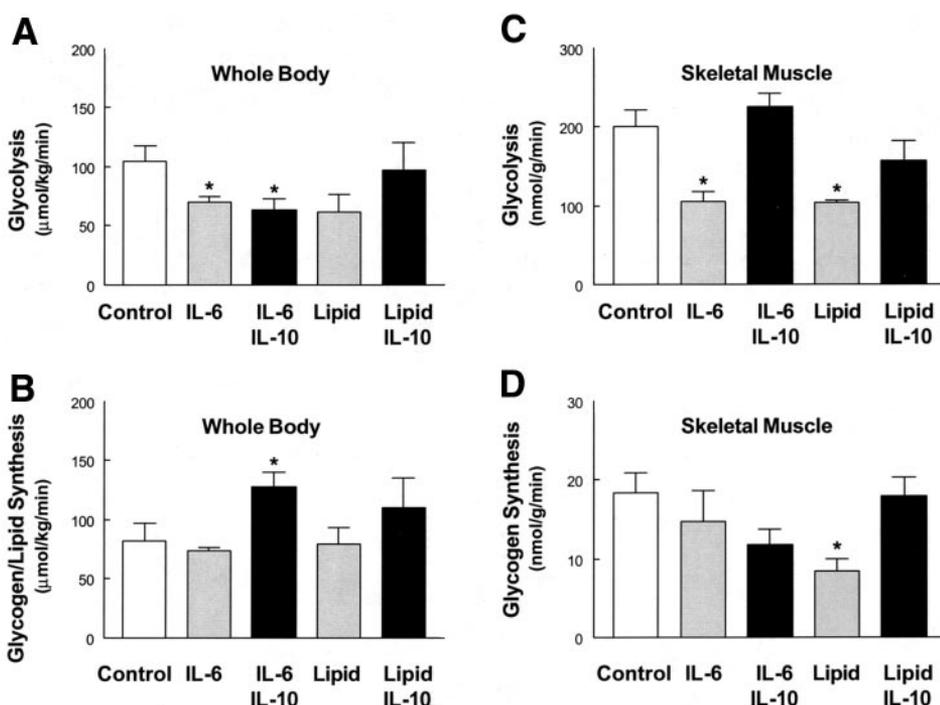

FIG. 2. Insulin-stimulated whole-body and skeletal muscle (gastrocnemius) glucose metabolic flux in the control, IL-6, IL-6/IL-10, lipid, and lipid/IL-10 mice. *A*: Insulin-stimulated whole-body glycolysis. *B*: Insulin-stimulated whole-body glycogen/lipid synthesis. *C*: Insulin-stimulated skeletal muscle glycolysis. *D*: Insulin-stimulated skeletal muscle glycogen synthesis. Values are means ± SE for five to eight experiments. *$P < 0.05$ vs. control mice.
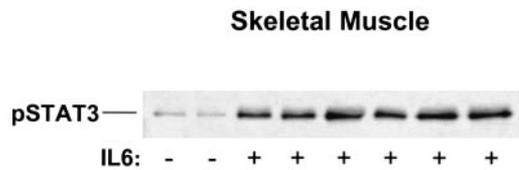
Skeletal Muscle

FIG. 3. Tyrosine phosphorylation of STAT3 in skeletal muscle (gastrocnemius) of saline or IL-6–treated mice.

remained reduced after co-treatment of IL-10 compared with the controls (Fig. 4D).

IL-10 prevented lipid-induced insulin resistance in skeletal muscle in vivo. Intralipid was infused for 5 h to raise circulating fatty acid levels (Table 1) and induce insulin resistance in skeletal muscle (23). As expected, lipid infusion significantly decreased insulin-stimulated whole-body and skeletal muscle glucose uptake (142 ± 12 and 83 ± 18 μmol $\cdot$ kg^{-1} $\cdot$ min^{-1} for whole-body glucose turnover and skeletal muscle glucose uptake, respectively) (Figs. 1 and 2). These changes were due to lipid-induced decreases in insulin-stimulated IRS-1–associated PI 3-kinase activity in skeletal muscle and were further associated with increased intramuscular fatty acyl-CoA levels (24 ± 11 nmol/g) (Fig. 1C and D). Co-treatment of IL-10 with lipid infusion did not affect circulating fatty acid levels, which remained elevated similar to the lipid-infused mice (Table 1). In contrast, IL-10 co-treatment completely prevented lipid-induced insulin resistance in skeletal muscle, as reflected by normal insulin-stimulated glucose uptake (181 ± 21 nmol $\cdot$ g^{-1} $\cdot$ min^{-1}) and insulin signaling in skeletal muscle (Fig. 1B and C). Additionally, this protective effect of IL-10 was associated with reduced intramuscular fatty acyl-CoA levels in the IL-10 co-treated with lipid mice (15 ± 2 nmol/g) compared with the lipid-infused mice (Fig. 1D). Neither lipid infusion nor lipid and IL-10 co-treatment affected hepatic insulin action, consistent with our previous results (23).

DISCUSSION

To examine the effects of IL-6 and IL-10 on tissue-specific insulin action, we performed 2-h hyperinsulinemic-euglycemic clamps after a 2-h IL-6, IL-10, or IL-6 and IL-10 co-treatment. Our findings showed that acute IL-6 treatment caused insulin resistance in skeletal muscle and liver that was associated with significant defects in insulin signaling and increases in intramuscular fatty acyl-CoA levels. Additionally, IL-6 treatment increased STAT3 tyrosine phosphorylation in skeletal muscle, suggesting the direct effects of IL-6 on skeletal muscle insulin resistance. In contrast, IL-10 co-treatment completely prevented IL-6–induced insulin resistance in skeletal muscle and liver. The protective effects of IL-10 were associated with normalization of insulin signaling and intramuscular fatty acyl-CoA levels. Moreover, IL-10 co-treatment prevented skeletal muscle insulin resistance mediated by a 5-h lipid infusion, and this effect was also associated with normal insulin signaling and intramuscular fatty acyl-CoA levels. Taken together, our findings demonstrated for the first time that acute IL-6 treatment caused skeletal muscle and hepatic insulin resistance in vivo and that IL-10 co-treatment prevented IL-6– and lipid-induced insulin resistance.

Previous studies have shown that IL-6 altered hepatic glucose metabolism (34,35). Ritchie (34) showed that overnight treatment of cultured rat hepatocytes with IL-6 increased labeled glucose release from prelabeled glycogen pools, whereas Kanemaki et al. (35) showed that IL-6 stimulated hepatic glycogen phosphorylase, a rate-limiting enzyme in glycogenolysis. Further supporting the effects of IL-6 to increase HGP, Senn et al. (17) recently found that IL-6 pretreatment reduced insulin-stimulated IRS-1 tyrosine phosphorylation as well as IRS-1–associated PI 3-kinase activity in isolated hepatocytes. In contrast to the potential effects of IL-6 on hepatic insulin resistance, Stouthard et al. (18) showed that IL-6 treatment increased glucose transport in 3T3-L1 adipocytes. Furthermore, Wal-
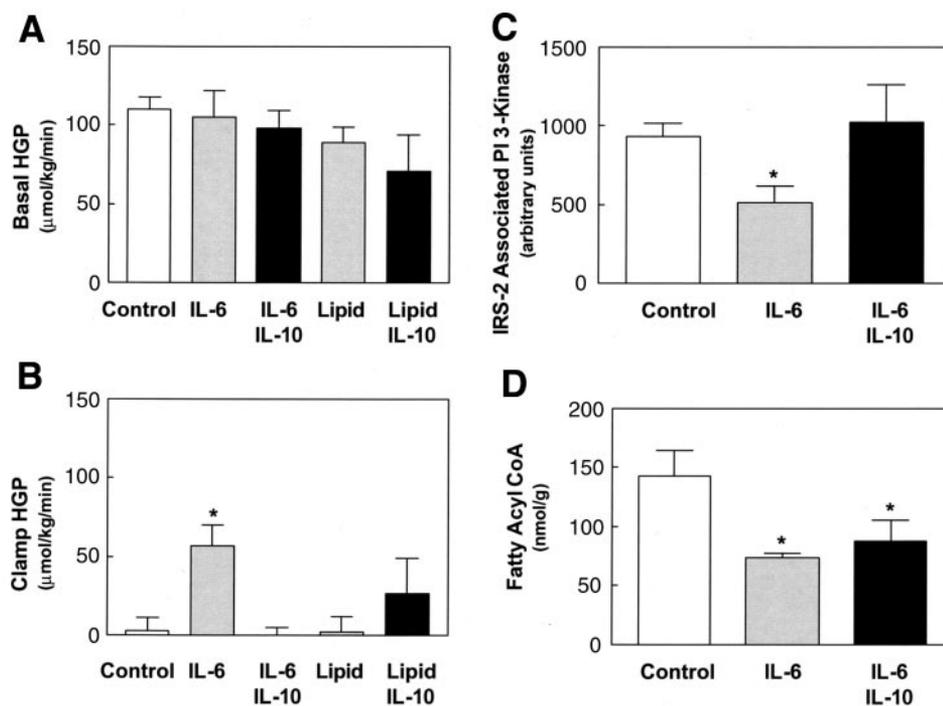

FIG. 4. Hepatic insulin action and fatty acyl-CoA levels in the control, IL-6, IL-6/IL-10, lipid, and lipid/IL-10 mice. *A*: Basal HGP. *B*: Clamp HGP. *C*: Insulin-stimulated IRS-2–associated PI 3-kinase activity in liver. *D*: Intrahepatic fatty acyl-CoA levels. Values are means ± SE for five to eight experiments. *P < 0.05 vs. control mice.
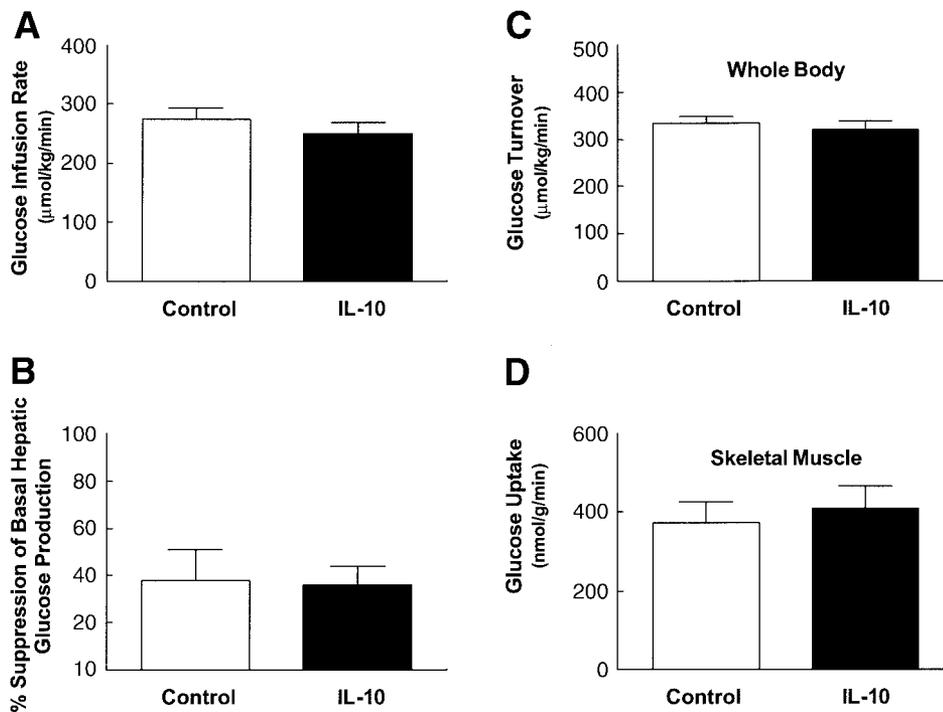
FIG. 5. Skeletal muscle and hepatic insulin action after IL-10 treatment in the control (○) and IL-10 (●) mice. *A*: Steady-state glucose infusion rate. *B*: Percent suppression of basal HGP. *C*: Insulin-stimulated whole-body glucose turnover in vivo. *D*: Insulin-stimulated glucose uptake in skeletal muscle (gastrocnemius) in vivo. Values are means ± SE for six to seven experiments.

lenius et al. (36) generated IL-6–deficient mice that were found to develop obesity and become glucose intolerant. Overall, it is clear that in vitro studies with IL-6 have yielded inconsistent results with regard to its effects on whole-body glucose homeostasis. Additionally, the effects of IL-6 on insulin action in skeletal muscle, quantitatively the most important insulin-responsive organ in the body (37), have not been previously examined.

The present findings demonstrated that IL-6 treatment significantly decreased insulin-stimulated glucose uptake in skeletal muscle in vivo, and the underlying mechanism involved defects in insulin-mediated IRS-1–associated PI 3-kinase activity, which is an important intracellular mediator of muscle insulin signaling (1). In addition to the IL-6–induced peripheral insulin resistance, IL-6 pretreatment also blunted insulin's ability to suppress basal HGP in vivo and insulin-mediated IRS-2–associated PI 3-kinase activity in the liver. The biological activities of IL-6 are initiated by binding to a high-affinity receptor complex, consisting of two membrane glycoproteins: the 80-kDa ligand binding component and 130-kDa signal-transducing component (gp130). Upon binding of IL-6, dimerization of gp130 is followed by activation of Janus-activated kinase, which promotes the tyrosine phosphorylation of gp130 (15). This event triggers the recruitment of signal-transducing molecules, such as SHP-2 and STAT3, leading to the activation of suppressor of cytokine signaling (SOCS)-3 (38–40). Recent studies have demonstrated the inhibitory effects of SOCS-3 on insulin-signaling molecules in isolated hepatocytes/HepG2 cells (41) and 3T3-L1 adipocytes (42,43), and the underlying mechanism may involve ubiquitin-mediated degradation of IRS-1 and IRS-2 proteins (44). To determine whether IL-6–mediated activation of STAT3 and SOCS-3 is involved in skeletal muscle insulin resistance, we determined the tyrosine phosphorylation of STAT3 in skeletal muscle of mice treated with

IL-6 for 10 min and found that IL-6 treatment profoundly increased tyrosine phosphorylation of STAT3 in skeletal muscle compared with the controls. The effects of IL-6–mediated STAT3 activation in skeletal muscle may be further supported by the findings of Zhang et al. (45) in which IL-6 was shown to increase IL-6 receptor expression in skeletal muscle. Overall, one hypothesis by which IL-6 caused skeletal muscle insulin resistance involves IL-6–induced activation of STAT3 and SOCS-3 in skeletal muscle, subsequently promoting SOCS-3–mediated degradation of IRS-1 and IRS-2 and leading to defects in insulin signaling and action.

An alternative hypothesis involves IL-6–induced increases in intramuscular fatty acyl-CoA levels. Previous studies have shown a strong inverse relationship between intramuscular fat content and insulin sensitivity in both animal models and humans (46–48). We have also demonstrated that muscle-specific overexpression of lipoprotein lipase, the rate-controlling enzyme in fatty acid uptake into cells (49), caused muscle-specific insulin resistance due to intramuscular accumulation of fatty acid–derived metabolites (47). The underlying mechanism may involve activation of serine kinase cascade, of which PKC-θ and/or IKK-β may play a role, by fatty acid–derived metabolites (e.g., fatty acyl-CoA) leading to the serine phosphorylation of IRS-1 (50–54). In this regard, Yuan et al. (52) have demonstrated that activation of IKK-β resulted in defects in skeletal muscle insulin signaling. Additionally, serine phosphorylation of IRS-1 has been shown to reduce tyrosine phosphorylation of IRS-1 and interfere with its ability to recruit and activate PI 3-kinase, as occurs upon treatment with TNF-α and okadaic acid (55,56). Thus, IL-6–induced insulin resistance in skeletal muscle may involve increases in intramuscular fatty acyl-CoA levels and their subsequent deleterious effects on insulin signaling and action. The mechanism by which IL-6 increases

intramuscular fat content is unknown but may involve increases in fatty acid uptake and/or decreases in fatty acid oxidation. Moreover, since IL-6 pretreatment did not raise intrahepatic fatty acyl-CoA levels, the mechanism by which IL-6 caused hepatic insulin resistance might involve activation of STAT3 signaling pathway and/or other fatty acid metabolites in liver.

Interestingly, we found that co-treatment of the anti-inflammatory cytokine IL-10 completely prevented IL-6–induced defects in both hepatic and skeletal muscle insulin action. The protective effects of IL-10 on IL-6–induced insulin resistance involved normalization of insulin signaling and reduction in intramuscular fatty acyl-CoA levels compared with the IL-6–treated mice. Moreover, we demonstrated that co-treatment of IL-10 also prevented lipid-induced defects in skeletal muscle insulin signaling and action, and this was associated with IL-10–mediated reduction in intramuscular fatty acyl-CoA levels. Since IL-10 prevented both IL-6–induced and lipid-induced insulin resistance in skeletal muscle, the underlying mechanism may involve a common pathway mediated by both IL-6 and lipid infusion. In this regard, we recently demonstrated that skeletal muscle insulin resistance induced by 5-h lipid infusion was due to increases in intramuscular fatty acyl-CoA levels, activation of PKC-θ, and subsequent defects in insulin signaling (57). Thus, we hypothesize that IL-6–induced insulin resistance in skeletal muscle is partly mediated via increases in intramuscular fatty acid–derived metabolites and by potential activation of PKC-θ and/or IKK leading to defects in insulin signaling and action. Furthermore, the protective effects of IL-10 on IL-6–induced and lipid-induced insulin resistance may involve IL-10–mediated decreases in intramuscular fatty acid–derived metabolites and/or direct inhibition of IKK. In contrast, because intrahepatic fatty acyl-CoA levels were reduced after IL-6 or IL-6/IL-10 co-treatment, different mechanisms may be responsible for cytokine-induced alteration in hepatic insulin action.

In conclusion, our findings, for the first time, demonstrate that IL-6 treatment causes insulin resistance in skeletal muscle and liver in vivo and that co-treatment of the anti-inflammatory cytokine IL-10 protects IL-6–induced and lipid-induced insulin resistance. These findings demonstrate the important role of IL-6 in the pathogenesis of insulin resistance and further implicate IL-10 as a potential therapeutic target in the treatment of insulin resistance.

REFERENCES

1. Kahn CR: Insulin action, diabetogenes, and the cause of type II diabetes. *Diabetes* 43:1066–1084, 1994
2. DeFronzo RA: The triumvirate: beta-cell, muscle, liver: a collusion responsible for NIDDM. *Diabetes* 37:667–687, 1988
3. Reaven GM: Role of insulin resistance in human disease. *Diabetes* 37:1595–1607, 1988
4. Boden G: Obesity, free fatty acids, and insulin resistance. *Curr Opin Endocr Diabetes* 8:235–239, 2001
5. Carr A, Samaras K, Burton S, Law M, Freund J, Chisholm DJ, Cooper DA: A syndrome of peripheral lipodystrophy, hyperlipidaemia, and insulin resistance in patients receiving HIV protease inhibitors. *AIDS* 12:F51–F58, 1998
6. Murata H, Hruz PW, Mueckler M: The mechanism of insulin resistance caused by HIV protease inhibitor therapy. *J Biol Chem* 275:20251–20254, 2000
7. Fogar P, Basso D, Pasquali C, Piva MG, Brigato L, De Paoli M, Galeotti F, Corsini A, Plebani M: Portal but not peripheral serum levels of interleukin-6 could interfere with glucose metabolism in patients with pancreatic cancer. *Clin Chim Acta* 277:181–189, 1998
8. Steppan CM, Bailey ST, Bhat S, Brown EJ, Banerjee RR, Wright CM, Patel HR, Ahima RS, Lazar MA: The hormone resistin links obesity to diabetes. *Nature* 409:307–312, 2001
9. Yamauchi T, Kamon J, Waki H, Terauchi Y, Kubota N, Hara K, Mori Y, Ide T, Murakami K, Tsuboyama-Kasaoka N: The fat-derived hormone adiponectin reverses insulin resistance associated with both lipoatrophy and obesity. *Nat Med* 7:941–946, 2001
10. Kahn CR, Chen L, Cohen SE: Unraveling the mechanism of action of thiazolidinediones. *J Clin Invest* 106:1305–1307, 2000
11. Hotamisligil GS, Shargill NS, Spiegelman BM: Adipose expression of tumor necrosis factor-alpha: direct role in obesity-linked insulin resistance. *Science* 259:87–91, 1993
12. Stouthard JM, Romijn JA, Van der Poll T, Endert E, Klein S, Bakker PJM, Veenhof CHN, Sauerwein HP: Endocrinologic and metabolic effects of interleukin-6 in humans. *Am J Physiol* 268:E813–E819, 1995
13. Pickup JC, Chusney GD, Thomas SM, Burt D: Plasma interleukin-6, tumor necrosis factor α and blood cytokine production in type 2 diabetes. *Life Sci* 67:291–300, 2000
14. Kern PA, Ranganathan S, Li C, Wood L, Ranganathan G: Adipose tissue tumor necrosis factor and interleukin-6 expression in human obesity and insulin resistance. *Am J Physiol* 280:E745–E751, 2001
15. Kishimoto T: The biology of interleukin-6. *Blood* 71:1–10, 1989
16. Greenberg AS, McDaniel ML: Identifying the links between obesity, insulin resistance, and β-cell function: potential role of adipocyte-derived cytokines in the pathogenesis of type 2 diabetes. *Eur J Clin Invest* 32:24–34, 2002
17. Senn JJ, Klover PJ, Nowak IA, Mooney RA: Interleukin-6 induces cellular insulin resistance in hepatocytes. *Diabetes* 51:3391–3399, 2002
18. Stouthard JM, Oude Elferink RPJ, Sauerwein HP: Interleukin-6 enhances glucose transport in 3T3–L1 adipocytes. *Biochem Biopys Res Comm* 220:241–245, 1996
19. Pedersen BK, Steensberg A, Schjerling P: Exercise and interleukin-6. *Curr Opin Hematol* 8:137–141, 2001
20. Fernandez-Real JM, Broch M, Vendrell J, Gutierrez C, Casamitjana R, Pugeat M, Richart C, Ricart W: Interlekin-6 gene polymorphism and insulin sensitivity. *Diabetes* 49:517–520, 2000
21. Vozarova B, Fernandez-Real JM, Knowler WC, Gallart L, Hanson RL, Gruber JD, Ricart W, Vendrell J, Richart C, Tataranni PA, Wolford JK: The interleukin-6(-174) G/C promotor polymorphism is associated with type-2 diabetes mellitus in Native Americans and Caucasians. *Hum Genet* 112:409–413, 2003
22. Cline GW, Petersen KF, Krssak M, Shen J, Hundal RS, Trajanoski Z, Inzucchi S, Dresner A, Rothman DL, Shulman GI: Impaired glucose transport as a cause of decreased insulin-stimulated muscle glycogen synthesis in type 2 diabetes. *N Engl J Med* 341:240–246, 1999
23. Kim JK, Kim Y-J, Fillmore JJ, Chen Y, Moore I, Lee J, Yuan M, Li ZW, Karin M, Perret P, Shoelson SE, Shulman GI: Prevention of fat-induced insulin resistance by salicylate. *J Clin Invest* 108:437–446, 2001
24. Yin M-J, Yamamoto Y, Gaynor RB: The anti-inflammatory agents aspirin and salicylate inhibit the activity of IκB kinase-β. *Nature* 396:77–80, 1998
25. Schottelius AJG, Mayo MW, Sartor RB, Baldwin AS: Interleukin-10 signaling blocks inhibitor of κB kinase activity and nuclear factor κB DNA binding. *J Biol Chem* 274:31868–31874, 1999
26. Van Exel E, Gussekloo J, De Craen AJ, Frolich M, Bootsma-Van Der Wiel A, Westendorp RG: Low production capacity of interleukin-10 associates with the metabolic syndrome and type 2 diabetes: the Leiden 85-Plus Study. *Diabetes* 51:1088–1092, 2002
27. Kim JK, Michael MD, Previs SF, Peroni OD, Mauvais-Jarvis F, Neschen S, Kahn BB, Kahn CR, Shulman GI: Redistribution of substrates to adipose tissue promotes obesity in mice with selective insulin resistance in muscle. *J Clin Invest* 105:1791–1797, 2000
28. Kim YB, Shulman GI, Kahn BB: Fatty acid infusion selectively impairs insulin action on Akt1 and protein kinase C λ/ζ but not on glycogen synthase kinase-3. *J Biol Chem* 277:32915–32922, 2002

29. Bligh EG, Dyer WJ: A rapid method of total lipid extraction and purification. *Can J Biochem Physiol* 37:911–917, 1959

30. Sandler S, Bendtzen K, Eizirik DL, Welsh M: Interleukin-6 affects insulin secretion and glucose metabolism of rat pancreatic islets in vitro. *Endocrinology* 126:1288–1294, 1990

31. Eizirik DL, Sandler S, Welsh N, Cetkovic-Cvrlje M, Nieman A, Geller DA, Pipeleers DG, Bendtzen K, Hellerstrom C: Cytokines suppress human islet function irrespective of their effects on nitric oxide generation. *J Clin Invest* 93:1968–1974, 1994

32. Stith RD, Luo J: Endocrine and carbohydrate response to interleukin-6 in vivo. *Circ Shock* 44:210–215, 1994

33. Previs SF, Withers DJ, Ren J-M, White MF, Shulman GI: Contrasting effects of IRS-1 *versus* IRS-2 gene disruption on carbohydrate and lipid metabolism *in vivo*. *J Biol Chem* 275:38990–38994, 2000

34. Ritchie DG: Interleukin 6 stimulates hepatic glucose release from prelabeled glycogen pools. *Am J Physiol* 258:E57–E64, 1990

35. Kanemaki T, Kitade H, Kaibori M, Sakitani K, Hiramatsu Y, Kamiyama Y, Ito S, Okumura T: Interleukin 1β and interleukin 6, but not tumor necrosis factor α, inhibit insulin-stimulated glycogen synthesis in rat hepatocytes. *Hepatology* 27:1296–1303, 1998

36. Wallenius V, Wallenius K, Ahren B, Rudling M, Carlsten H, Dickson SL, Ohlsson C, Jansson J-O: Interleukin-6 deficient mice develop mature-onset obesity. *Nat Med* 8:75–79, 2002

37. Baron AD, Brechtel G, Wallace P, Edelman SV: Rates and tissue sites of non-insulin- and insulin-mediated glucose uptake in humans. *Am J Physiol* 255:E769–E774, 1988

38. Lutticken C, Wegenka UM, Yuan J, Buschmann J, Schindler C, Ziemiecki A, Harpur AG, Wilks AF, Yasukawa K, Taga T: Association of transcription factor APRF and protein kinase Jak1 with the interleukin-6 signal transducer gp130. *Science* 263:89–92, 1994

39. Akira S, Nishio Y, Inoue M, Wang XJ, Wei S, Matsusaka T, Yoshida K, Sudo T, Naruto M, Kishimoto T: Molecular cloning of APRF, a novel IFN-stimulated gene factor 3p91-related transcription factor involved in the gp130-mediated signaling pathway. *Cell* 77:63–71, 1994

40. Yamanaka Y, Nakajima K, Fukada T, Hibi M, Hirano T: Differentiation and growth arrest signals are generated through the cytoplasmic region of gp130 that is essential for Stat3 activation. *EMBO J* 15:1557–1565, 1996

41. Senn JJ, Klover PJ, Nowak IA, Zimmers TA, Koniaris LG, Furlanetto RW, Mooney RA: Suppressor of cytokine-signaling-3 (SCOS-3), a potential mediator of interleukin-6-dependent insulin resistance in hepatocytes. *J Biol Chem* 278:13740–13746, 2003

42. Emanuelli B, Peraldi P, Filloux C, Sawka-Verhelle D, Hilton D, Van Obberghen E: SOCS-3 is an insulin-induced negative regulator of insulin signaling. *J Biol Chem* 275:15985–15991, 2000

43. Emanuelli B, Peraldi P, Filloux C, Chavey C, Freidinger K, Hilton DJ, Hotamisligil GS, Obberghen EV: SOCS-3 inhibits insulin signaling and is up-regulated in response to tumor necrosis factor-α in the adipose tissue of obese mice. *J Biol Chem* 276:47944–47949, 2001

44. Rui L, Yuan M, Frantz D, Shoelson S, White MF: SOCS-1 and SOCS-3 block insulin signaling by ubiquitin-mediated degradation of IRS1 and IRS2. *J Biol Chem* 277:42394–42398, 2002

45. Zhang Y, Pilon G, Marette A, Baracos VE: Cytokines and endotoxin induce cytokine receptors in skeletal muscle. *Am J Physiol* 279:E196–E205, 2000

46. Boden G, Lebed B, Schatz M, Homko C, Lemieux S: Effects of acute changes of plasma free fatty acids on intramyocellular fat content and insulin resistance in healthy subjects. *Diabetes* 50:1612–1617, 2001

47. Kim JK, Fillmore JJ, Chen Y, Yu C, Moore IK, Pypaert M, Lutz EP, Kako Y, Velez-Carrasco W, Goldberg IJ, Breslow JL, Shulman GI: Tissue-specific overexpression of lipoprotein lipase causes tissue-specific insulin resistance. *Proc Natl Acad Sci U S A* 98:7522–7527, 2001

48. Perseghin G, Scifo P, De Cobelli F, Pagliato E, Battezzati A, Arcelloni C, Vanzulli A, Testolin G, Pozza G, Del Maschio A: Intramyocellular triglyceride content is a determinant of in vivo insulin resistance in humans: a ^{1}H-^{13}C nuclear magnetic resonance spectroscopy assessment in offspring of type 2 diabetic patients. *Diabetes* 48:1600–1606, 1999

49. Bjorntorp P: Obesity. *Lancet* 350:423–426, 1997

50. Shulman GI: Cellular mechanisms of insulin resistance: *J Clin Invest* 106:171–176, 2000

51. Itani SI, Zhou Q, Pories WJ, MacDonald KG, Dohm GL: Involvement of protein kinase C in human skeletal muscle insulin resistance and obesity. *Diabetes* 49:1353–1358, 2000

52. Yuan M, Konstantopoulos N, Lee J, Hansen L, Li ZW, Karin M, Shoelson SE: Reversal of obesity- and diet-induced insulin resistance with salicylates or targeted disruption of IKK-beta. *Science* 293:1673–1677, 2001

53. Griffin ME, Marcucci MJ, Cline GW, Bell K, Barucci N, Lee D, Goodyear LJ, Kraegen EW, White MF, Shulman GI: Free fatty acid-induced insulin resistance is associated with activation of protein kinase C θ and alterations in the insulin signaling cascade. *Diabetes* 48:1270–1274, 1999

54. Chalkley SM, Hettiarachchi M, Chisholm DJ, Kraegen EW: Five-hour fatty acid elevation increases muscle lipids and impairs glycogen synthesis in the rat. *Metabolism* 47:1121–1126, 1998

55. Rui L, Aguirre V, Kim JK, Shulman GI, Lee A, Corbould A, Dunaif A, White MF: Insulin/IGF-1 and TNF-α stimulate phosphorylation of IRS-1 at inhibitory Ser[307] via distinct pathways. *J Clin Invest* 107:181–189, 2001

56. Pederson TM, Kramer DL, Rondinone CM: Serine/threonine phosphorylation of IRS-1 triggers its degradation: possible regulation by tyrosine phosphorylation. *Diabetes* 50:24–31, 2001

57. Yu C, Chen Y, Cline GW, Zhang D, Zong H, Wang Y, Bergeron R, Kim JK, Cushman SW, Cooney GJ, Atcheson B, White MF, Kraegen EW, Shulman GI: Mechanism by which fatty acids inhibit insulin activation of insulin receptor substrate-1 (IRS-1)-associated PI 3-kinase activity in muscle. *J Biol Chem* 277:50230–50236, 2002